

Near-to-node modal identification using multiple related response models

Miha Pogačar^a, Tomaž Bregar^b, Gregor Čepon^{a,*}, Miha Boltežar^a

^a *University of Ljubljana, Faculty of Mechanical Engineering, Aškerčeva 6, 1000 Ljubljana, Slovenia*

^b *Gorenje d. o. o., Partizanska 12, 3503 Velenje, Slovenia*

Cite as:

Miha Pogačar, Tomaž Bregar, Gregor Čepon, Miha Boltežar, Near-to-node modal identification using multiple related response models, Measurement, 2020, <https://doi.org/10.1016/j.measurement.2020.108793>

Abstract

Experimental modal analysis (EMA) is a well-established procedure for determining the modal parameters of a structure. Typically, a point-force is used to excite the structure and the translational response is measured. When performing an EMA, problems with a reliable modal-parameter estimation can arise whenever a selected reference point is located in the proximity of a node for any mode shape in interest. This problem can be addressed by performing multi-reference measurements; however, a non-coincidental position with respect to the remaining nodes cannot be guaranteed. In this research a novel modal-identification method, based on multiple related experimental response models at a single reference point, is proposed as an alternative to the established multi-reference measurement. The idea is to combine multiple response models of the same structure, acquired by different types of sensors (e.g., translational and rotational) for which the nodes of the response-related modal shapes do not coincide. The Least-Squares Frequency-Domain (LSFD) method is modified by considering the mutual relations of the acquired response models. The proposed methodology is experimentally validated on a homogeneous aluminium beam.

*Corresponding author

Email address: gregor.cepon@fs.uni-lj.si (Gregor Čepon)

The proposed method shows both a successful modal identification and an increased consistency of the identified modal constants, despite the proximity of the nodes to the selected reference point.

Keywords: experimental modal analysis, related response models, hybrid LSFD, rotational degrees of freedom

1. Introduction

Experimental modal analysis is a reliable method for determining the true modal parameters of a structure, despite the remarkable advances in numerical simulation. First, the frequency response is measured at several points of the structure. Typically, a point-force excitation is performed with a modal hammer or an electrodynamic shaker [1]. In addition, various techniques such as moment [2, 3] or air-pressure-induced excitation [4] are also possible. The response is usually measured with translational sensors (e.g., a piezo-electric accelerometer [5], a laser vibrometer [6], a high-speed camera [7]), although rotational [8, 9] or strain measurements [10, 11] can also be performed. Based on the acquired response model, the modal parameters (i.e., the natural frequencies, damping ratios and mode shapes) are identified. When analysing real structures, advanced modal-identification methods, such as the Least-Squares Complex-Frequency (LSCF) [12, 13] and the Least-Squares Frequency-Domain (LSFD) [14] methods are often applied, as they can also be used with relatively noisy and inconsistent data sets [15].

Another approach to determining the dynamic properties of structures is operational modal analysis (OMA), where only the output is being measured. This is convenient for several practical applications. Therefore, various methods were developed to address the issues of output-only modal identification, such as Modified Sparse Component Analysis by the Time-Frequency Method (SCA-TF) [16] and the Frequency Domain Independent Component Analysis (ICA-F) method [17]. Furthermore, the problem of closely spaced modes was addressed in [18]. Output-only modal analysis is not a subject of this paper; however,

some approaches presented are also applicable in the scope of OMA.

Within the paper, the full response model is considered as a set of FRFs, obtained for every possible combination of the response and the excitation location for a given discretized structure. When performing a classic EMA, a single row or column of a full response model is theoretically sufficient to identify all the modal parameters of a structure [1]. In order to obtain a single row, the excitation is performed at multiple points, while the response is only measured at a selected reference point. The procedure is reversed if a column measurement is considered. However, when performing an EMA on real complex structures, with the modal shapes still unknown, it is not uncommon for a selected reference point to be placed in the proximity of a node for at least one of the significant vibration modes. As a result, poorly detectable resonance peaks appear in the measured frequency response functions (FRFs). These peaks are greatly affected by noise and other measurement uncertainties. For highly uncertain resonance peaks, problems with a reliable modal-parameter estimation can occur, even with the use of advanced methods, such as LSCF/LSFD [7]. Furthermore, problems with a consistent mass normalization of the modal shapes can occur, which is crucial for inferring the mass and stiffness properties of the system.

Several methods were developed to address the problem of optimum sensor placement. The driving-point residue method was presented in [19] and an effective independence method was proposed in [20]. Information entropy was used to measure the uncertainty of the model parameter estimates in [21], and large finite-element models were addressed in [22]. However, all the listed methods are based on a analytical or numerical model of the system under consideration, which is not always available. Moreover, when dealing with complex real structures, an arbitrary (optimum) reference point might not be accessible or the sensor placement/excitation might not be physically possible. The problem proves to be even more complex when a purely experimental approach is considered. Sometimes, it is practically impossible to find a suitable single reference point to identify all the modes of interest [1]. In such a case, a multi-reference measurement has to be performed; however, a non-coincidental position with

respect to any of the remaining nodes cannot be guaranteed.

In this paper a novel hybrid methodology for modal-parameter identification on near-to-node obtained response models is proposed. Instead of performing multi-reference measurements, multiple related response models of the same structure are obtained at a single reference point. The presented approach is based on a combined measurement, using different types of sensors, for which the nodes of the response-related modal shapes do not coincide. Thus, adequately detectable resonance peaks are available for all vibration modes and a consistent LSCF complex-eigenvalue identification can be performed. Further, the standard LSFD method is modified by taking into account the mutual relationships of the acquired response models. By using a proposed hybrid LSFD method, the consistency of the estimated low-response-related modal constants can be increased. Finally, an experimental study was performed, analysing the bending vibration modes with a combined translational and rotational response measurement. Compared to the standard LSFD method, a significant improvement in the consistency of the modal constants is demonstrated when the mode shapes reflect the node's proximity to the selected reference point. As a result, the accuracy of the identified mass-normalized mode shapes and the noise-dominant areas of the reconstructed FRFs is increased.

This paper is organized as follows. The next section summarizes the basic theory of related response and modal models, followed by an overview of the modal parameter estimation (MPE) methods. In Section 3 the proposed hybrid methodology for near-to-node MPE is outlined. In Section 4 the methodology is validated on a laboratory experimental setup. Finally, conclusions are drawn in Section 5.

2. Theoretical background

2.1. Response model

In experimental modal analysis, the response of a structure is typically obtained in the form of frequency response functions. For a linear and time-

invariant mechanical system in the steady state, the equation of motion in the frequency domain can be given as:

$$\mathbf{X}(\omega) = \mathbf{H}(\omega) \mathbf{F}(\omega), \quad (1)$$

where \mathbf{X} represents a response (labeled with index r) vector, whose length is equal to the number of selected response points n_r . Further, \mathbf{F} denotes an excitation (labeled with index e) vector of length n_e , being equal to the number of selected excitation points and \mathbf{H} is a $n_r \times n_e$ matrix of frequency response functions. For a general viscously damped system with N degrees of freedom, a response model can be formulated as [23]:

$$\mathbf{H}(\omega) = \sum_{r=1}^N \left(\frac{{}_r\mathbf{A}}{i\omega - \lambda_r} + \frac{{}_r\mathbf{A}^*}{i\omega - \lambda_r^*} \right), \quad (2)$$

with the asterisk denoting the value of the complex conjugate, i being the unit imaginary number and ${}_r\mathbf{A}$ denoting a $n_r \times n_e$ matrix of modal constants¹. The system complex eigenvalue λ_r or the so-called pole contains information about the natural frequency ω_r and the damping ratio ζ_r at the r -th vibration mode:

$$\lambda_r = -\zeta_r \omega_r \pm i\omega_r \sqrt{1 - \zeta_r^2}. \quad (3)$$

The matrix of modal constants ${}_r\mathbf{A}$ is equivalent to the outer product of the normalized mode shapes ${}_r\Phi^r$ and ${}_r\Phi^e$, where the former is related to the response and the latter to the excitation type of physical quantity.

In the case of a complementary excitation-response pair, e.g., force-displacement or moment-rotation, the two mode shapes are identical. Therefore, the indices e and r can be omitted, resulting in a symmetrical matrix:

¹It should be noted that for a general viscously damped model, modal constants ${}_r\mathbf{A}$ (also being called residues) are not equal to the modal constants from a hysteretically damped models and are also subjected to different normalization [23, 24].

$${}_r \mathbf{A}^{\text{com}} = \begin{bmatrix} \phi_{1r} \phi_{1r} & \cdots & \phi_{1r} \phi_{kr} & \cdots & \phi_{1r} \phi_{n_e r} \\ \vdots & \ddots & \vdots & \ddots & \vdots \\ \phi_{jr} \phi_{1r} & \cdots & \phi_{jr} \phi_{kr} & \cdots & \phi_{jr} \phi_{n_e r} \\ \vdots & \ddots & \vdots & \ddots & \vdots \\ \phi_{n_r r} \phi_{1r} & \cdots & \phi_{n_r r} \phi_{kr} & \cdots & \phi_{n_r r} \phi_{n_e r} \end{bmatrix}, \quad (4)$$

As can be deduced from Equation (4), all the rows and columns are proportional to the r -th mode shape. Therefore, it is theoretically sufficient to measure a single row or column of the modal constants in order to identify all the modal parameters. However, in the case of a non-complementary excitation-response pair, e.g., force-rotation or force-strain, the formulation of modal constants matrix exhibits non-symmetrical properties [11]:

$${}_r \mathbf{A}^{\text{ncom}} = \begin{bmatrix} \phi_{1r}^r \phi_{1r}^e & \cdots & \phi_{1r}^r \phi_{kr}^e & \cdots & \phi_{1r}^r \phi_{n_e r}^e \\ \vdots & \ddots & \vdots & \ddots & \vdots \\ \phi_{jr}^r \phi_{1r}^e & \cdots & \phi_{jr}^r \phi_{kr}^e & \cdots & \phi_{jr}^r \phi_{n_e r}^e \\ \vdots & \ddots & \vdots & \ddots & \vdots \\ \phi_{n_r r}^r \phi_{1r}^e & \cdots & \phi_{n_r r}^r \phi_{kr}^e & \cdots & \phi_{n_r r}^r \phi_{n_e r}^e \end{bmatrix}, \quad (5)$$

where ϕ_{jr}^r and ϕ_{kr}^e are the components of the mode shapes ${}_r \Phi^r$ and ${}_r \Phi^e$, with the indices j and k referring to the corresponding excitation and response points on the structure, respectively. In this case it can be seen, that the rows and columns of the modal matrix are proportional to the excitation and r -th response-related mode shape, respectively.

2.2. Experimental modal-parameter estimation

When the dynamics of a structure is obtained experimentally, one typically measures its frequency response for several inputs and outputs. Whenever a response and excitation point coincide on the structure, the obtained FRF is referred to as a driving-point function or a transfer function when the two differ. In general, the dimensions of the acquired response model $\mathbf{H}(\omega)$ are arbitrary, whereas only an appropriate spatial resolution of the selected points is required

to identify the mode shapes of interest. An experimental process to obtain either an individual row or a column of the response model is shown in Figure 1.

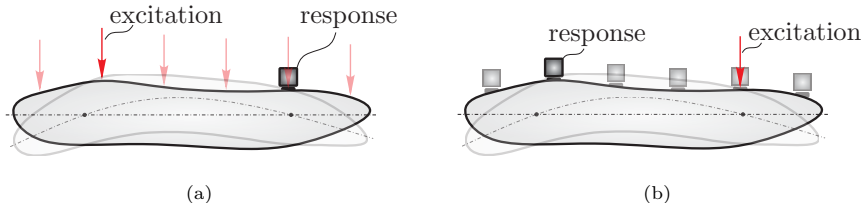


Figure 1: Measurement of a response model: (a) Row; (b) Column.

Following the procedure in [24] and considering Eq. (5), mass-normalized mode shapes can be determined from an arbitrary row or column of the response model and only the appropriate complex scaling is to be performed. Unlike in common practice with a complementary response-excitation sensor pair, different types of mode shapes are obtained from a row or column, respectively, when using a non-complementary sensor pair [25]. A comparison of the presented approaches is shown in Figure 2, referring to the combination of translational and rotational response measurements and the point-force excitation.

One of the important features of an identified modal shape is the number and the location of the corresponding nodes. A node is defined as a point with zero amplitude for a certain modal shape. Whether a suitable combination of sensors is used to perform the EMA, e.g., a translational and rotational sensor or a translational and a strain sensor, the nodes of the individual response-related modal shapes typically do not coincide. According to the principles of continuum mechanics [26], the rotational components are conditioned by the off-diagonal elements of the deformation gradient. Assuming that the reference point, if located in the proximity of the local minimum of the displacement field, a pronounced rotational response can therefore be expected. Accordingly, the translational and rotational mode shapes can be expected to have complementary properties in the case of a transverse response. Greater generality could be achieved by introducing the deformation sensors, since they can be used to measure both the normal and the shear components of the deformation tensor.

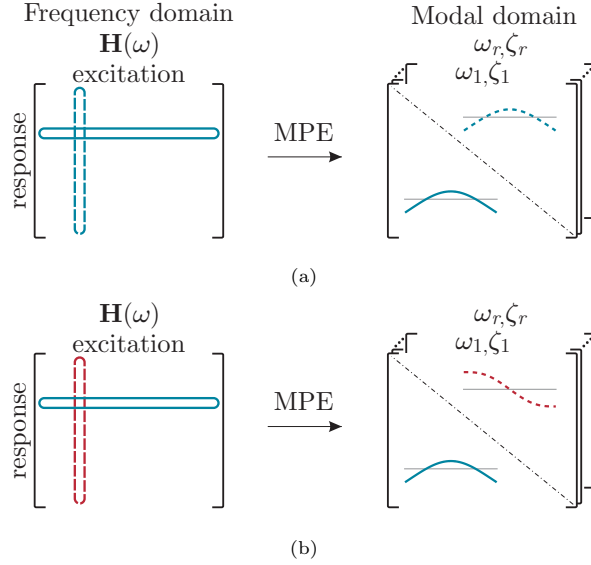


Figure 2: Response-excitation pair type: (a) Complementary; (b) Non-complementary.

Several MPE methods are available, such as the Ewins-Gleeson or the Complex Exponential method [23, 27]. However, when dealing with relatively noisy and inconsistent data [15], more advanced methods such as the Least-Squares Complex-Frequency (LSCF) [12, 13] and Least-Squares Frequency-Domain (LSFD) [14] methods are commonly used. The governing natural frequencies and damping ratios represent the global properties of the structure, so the same values are expected to be estimated for each response or excitation point. When performing a LSCF, a least-squares criterion is used to estimate the corresponding complex values and the true eigenvalues are then hand-picked from the stabilization diagram.

The complete dynamic information about a system, including the full series of vibration modes, is available solely for analytical or numerical models. When the dynamics of a structure is obtained experimentally, only a finite set of vibration modes is obtained due to the limited frequency range. The acquisition of the dynamic response above and below certain limits is not possible. However,

it significantly affects the FRF synthesis, and therefore an extension of Eq. (2) with the lower \mathbf{A}_L and upper residuals \mathbf{A}_U is required:

$$\mathbf{H}(\omega) = \sum_{r=1}^N \left(\frac{r\mathbf{A}}{i\omega - \lambda_r} + \frac{r\mathbf{A}^*}{i\omega - \lambda_r^*} \right) - \frac{\mathbf{A}_L}{\omega^2} + \mathbf{A}_U. \quad (6)$$

The set of identified poles from the LSCF is used in the LSFD, to estimate the values of the modal constants $r\mathbf{A}$ together with the lower and upper residuals \mathbf{A}_L and \mathbf{A}_U . This is performed by minimizing the deviation between the measured FRFs and the output of Eq. (6) for every component of the response model separately.

3. Modal-parameter estimation on multiple related response models

Whenever a selected reference point is located in the proximity of a node, for at least one of the mode shapes of interest, a reliable estimation of the corresponding modal parameters is difficult. A unique definition of the permissible proximity of a node is difficult to define, as it is influenced by several factors, such as the noise level, the damping ratio and the intensity of the excitation. The appropriateness of a chosen reference point is usually verified by the quality of a driving-point measurement. However, when analysing complex real structures with a high modal density, the proper selection of a single reference point can prove to be challenging or even impossible [1].

As an example, a numerical model of a washing machine's side panel is presented in Figure 3, exhibiting the node-proximity problems. The boundary conditions on the model simulate the fastening with four screws at the panel corners. The selected impact and sensor location is given in Figure 3a. In the frequency range up to 120 Hz, the amplitude spectra of the translational FRF (Figure 3b) exhibits a low response at the 3rd (75 Hz) and the 6th (105 Hz) mode, implying the node's proximity to the selected reference point. This can be confirmed by examining the mode shapes in Figure 3c. However, we can observe that at least one of the rotational responses provides a reliable high amplitude reading.

Therefore, instead of changing the position of a reference point, the type of excitation or response can be changed when measuring the row or the column of a full response model, respectively. Since the nodes of different types of mode shapes typically do not coincide, such a technique might prove to be a preferable solution in order to avoid the node-proximity problems.

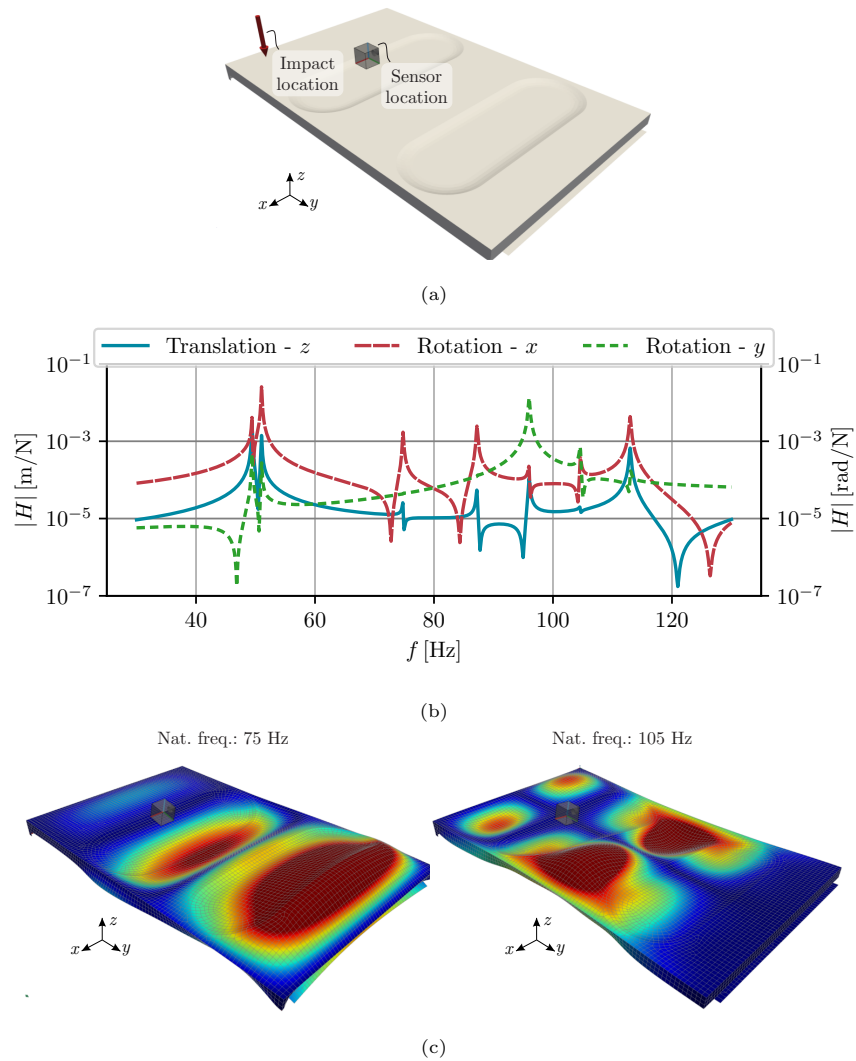


Figure 3: Numerical model of a washing machine's side panel: (a) Numerical model; (b) Translational and rotational FRFs for the given impact and sensor location; (c) Mode shapes at 3rd and 6th natural frequency.

The following proposed methodology is limited to the case where the response model of a structure is obtained as a single row, which is common practice in the field of impact-excitation-based EMA [1]. However, the same concept can be applied with single-column measurements when using different types of excitation. Having the j -th point denoted as the reference point, the corresponding matrix of the modal constants for the r -th vibration mode (Eq. (5)) can be formulated as a single row:

$${}_r\bar{\mathbf{A}}^{\text{ncom}} = (\phi_{j_r}^r {}_r\Phi^e)^T \quad (7)$$

In the proximity of a node for the r -th response-related vibration mode, the corresponding eigenvector element $\phi_{j_r}^r$ approaches a value of zero. As a result, a complete row of estimated modal constants (MCs) consists of low numerical values, which leads to difficulties with a reliable MPE.

The proposed methodology is generally applicable. However, in order to provide a clear representation, a further analysis on bending vibration modes is presented, using a combination of translational and rotational response measurements. In addition, such a reference point is selected so that difficulties associated with the proximity of the node are alternately reflected in the translational and rotational mode shapes.

The proposed novel procedure for a modal-parameter estimation consists of six main steps, which are presented in Figure 4. In the proposed procedure, LSCF [12, 13]/LSFD [14] methods are used for primary identification. However, other identification methods may be used if considered more suitable in a given case, e.g. methods [28, 29] whether closely spaced modes are considered.

- **STEP 1: Measurement**

Multiple related single-row response models are obtained at a selected reference point, using different types of sensors. Here, the used set of sensors is presumed to follow the assumption of non-coincidental node locations at the corresponding response-related mode shapes.

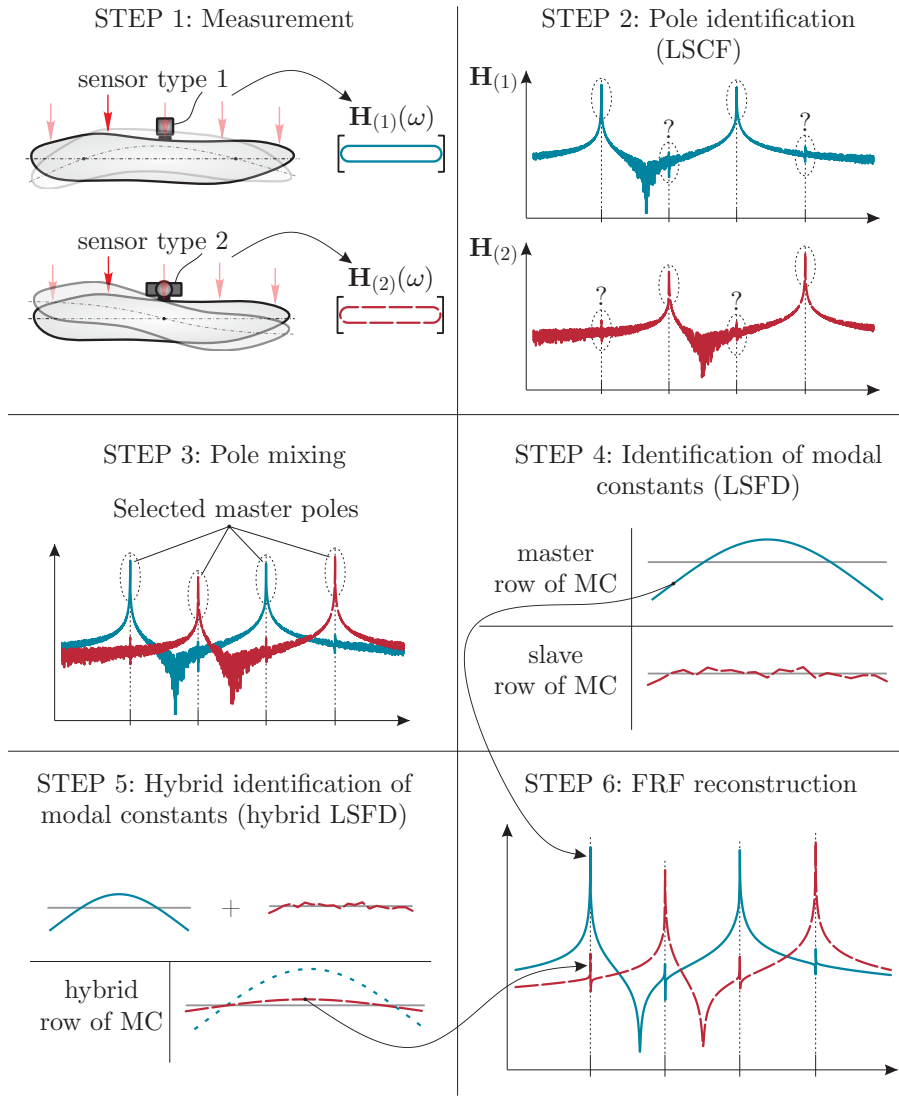


Figure 4: Proposed procedure for modal parameter estimation on multiple response models.

- **STEP 2:** Pole identification

For each individual response model, an LSCF identification of the complex-eigenvalues (also called poles) is performed. Poorly detectable resonance peaks (**slave peaks**) occur at resonances for which the response-related mode shapes reflect the node's proximity to the selected reference point.

The identification of the corresponding poles (**slave poles**) is therefore greatly affected by noise and other measurement uncertainties, leading to inconsistent estimates or even the absence of any pole stabilization.

In cases, when the same resonant peaks are easily detectable with different sensors, the proposed method does not presuppose any special procedure. It is advisable to use the results obtained with the sensor having superior metrological specifications, which is typically the translational accelerometer.

- **STEP 3:** Pole mixing

However, having additional response models with non-coincidental mode-shape nodes, adequately detectable resonance peaks (**master peaks**) are available for all the vibration modes. Therefore, a set of reliable poles (**master poles**) can be formed by combining the poles from different sensors.

- **STEP 4:** Identification of modal constants

The selected set of master poles is applied to the standard LSFD method, in order to estimate the unknown modal constants for all the vibration modes, including the lower and upper residuals for each response model. With such an approach, the estimation of relevant slave-peak-related modal constants is possible; however, a significant effect of measurement uncertainties can also be observed [7].

- **STEP 5:** Hybrid identification of modal constants

When multiple response models are available, the identification of slave-peak-related modal constants (**slave rows of MCs**) can be improved by considering the relationship with the master-peak-related modal constants (**master rows of MCs**) from another sensor with the use of the proposed hybrid LSFD method.

In compliance with Eq. (7), two distinct, single-row response models, obtained using the selected sensors are proportional. Therefore, the relation

between a master and a slave row of the modal constants at the r -th vibration mode, acquired by two distinct sensors, can be formulated as:

$$\frac{{}_r\bar{\mathbf{A}}^s}{{}_r\bar{\mathbf{A}}^m} = {}_r p, \quad (8)$$

where the master and slave indices are labelled as m and s, respectively, and ${}_r p$ is the corresponding (unknown) complex scaling factor. A matrix system of equations for the LSFD method can be formulated as:

$$\mathbf{H}_{\text{exp}} = \mathbf{P} \mathbf{A}, \quad (9)$$

where \mathbf{H}_{exp} represents a matrix of the experimental FRFs, \mathbf{P} is a matrix containing pole-dependent denominators and \mathbf{A} is a global matrix of unknowns. The standard LSFD method is based on a local optimization process, performed in compliance with Eq. (6). Each of the columns in matrix \mathbf{A} , composed of modal constants and the corresponding lower and upper residuals, is obtained separately for an individual FRF. The individual rows in the matrix of the unknown modal constants are thus arranged in a sequence of vibration modes. Whenever the row in a particular sensor is related to the more reliable resonant peak it is denoted as a master row, whereas the row at the same mode is denoted as a slave row for the other sensor.

In the case of a hybrid LSFD, for each individual sensor the slave rows of the uncorrelated unknowns in matrix \mathbf{A} can be replaced (Figure 5). The replaced row can be obtained using Eq. (8) by scaling the related master row of MCs from another sensor. The resulting r -th hybrid row is therefore proportional to the r -th master row of MCs, whereby in the least-squares procedure the proportionality factor ${}_r p$ is obtained. With such a modification, a global optimization is implemented instead of a local one, which reduces the influence of the inconsistencies between the individual FRFs.

In addition, a mass normalization can be performed to obtain the modal shapes. It should be noted, however, that this process is relatively simple,

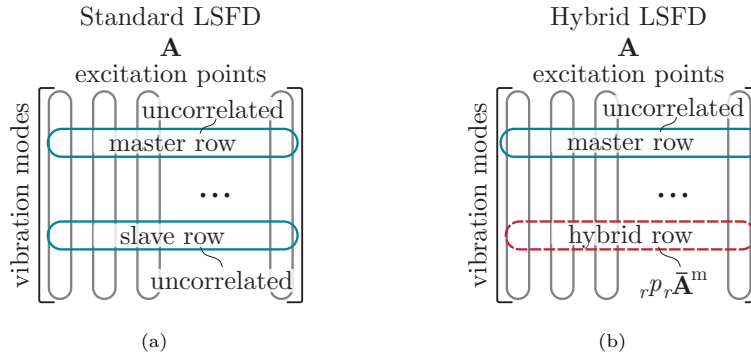


Figure 5: LSF method: (a) Standard; (b) Hybrid.

if at least one complementary response-excitation pair is used (see [24] and Eq. (5)) whereas a more complex experimental approach is required if only non-complementary response-excitation pairs are available [11].

- **STEP 6:** FRF reconstruction

Finally, a reconstruction of the FRFs for all the response models can be performed according to Eq. (6). Here, the set of selected master poles and estimated constants acquired by the hybrid LSF are applied.

4. Experimental study

An experimental study was performed on a solid aluminium beam with dimensions of $15 \times 40 \times 1000 \text{ mm}^3$, as shown in Figure 6. Approximately free-free boundary conditions were provided by the polyurethane-foam support blocks. An automated modal hammer with a brass tip was used to excite the structure at 51 equidistant points. The response of the beam was measured using a Dytran 3097A1 uniaxial translational accelerometer and a Kistler 8840 rotational accelerometer. Sensors were mounted at the centroid of the upper and lower beam surfaces, alternately providing low response measurements due to the proximity of the wave-nodes over the whole range of bending vibration modes.

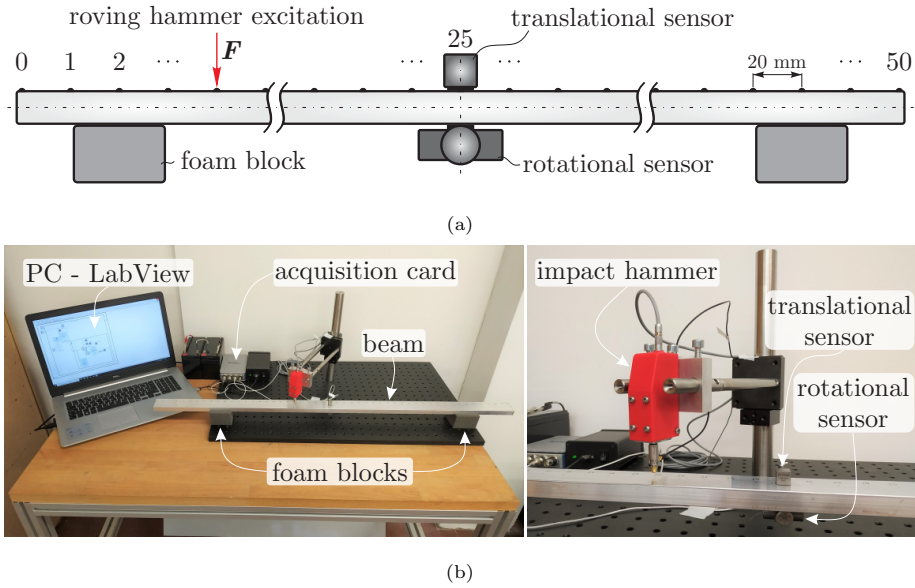


Figure 6: Experimental setup: (a) Schematic depiction; (b) Photograph.

4.1. Rotational sensor

A Kistler 8840 direct piezoelectric rotational accelerometer (Figure 7) was used to measure the angular motion of the beam. The sensor design is based on two spatially separated, quartz, shear-mode element assemblies [30], optimized for a low cross-axis sensitivity and base strain effects.



Figure 7: Rotational accelerometer [30].

4.2. Automated modal hammer

One of the key preconditions for an appropriate MPE is to ensure a proper structure excitation. Typically, hand-guided modal hammers are used, whereby the impact intensity, direction and position vary with every hit, thus increasing the bias and lowering the coherence of the measured FRFs. In order to avoid

such problems, an automated modal hammer *AMImpact* [31], shown in Figure 8, was used. Combined with a rigid support structure, it enabled a highly repetitive excitation at a precise position on the structure under study.



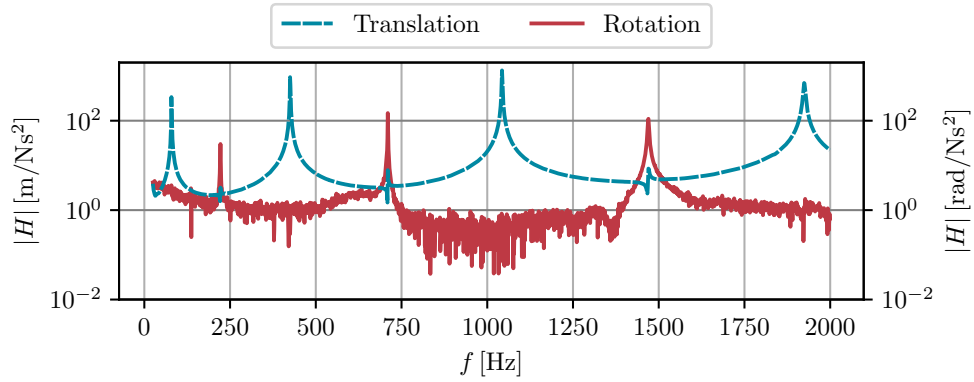
Figure 8: Automated modal hammer.

4.3. Step 1: Measurement

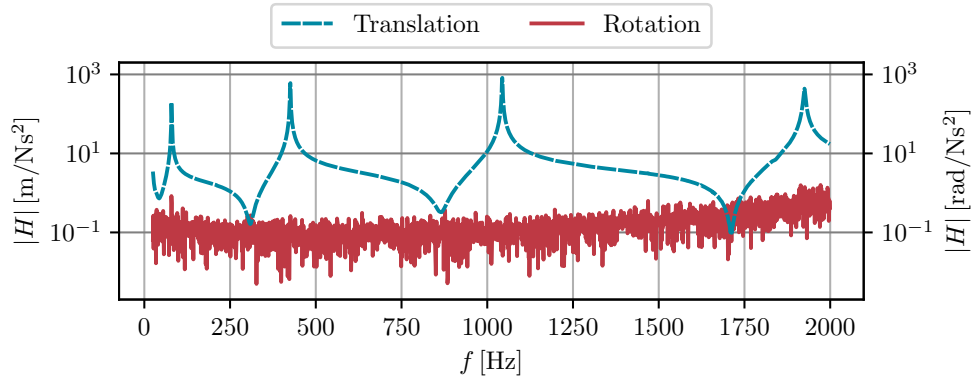
Translational and rotational accelerances at each of the 51 points on the beam were acquired from ten individual impact-response measurements. The amplitude spectra of the accelerances at points 0 and 25 are shown in Figure 9. The response was analysed in the range from 25 to 2000 Hz, the lower limit being set by the foam block's natural frequency and the upper limit being set by the calibration range of the rotational accelerometer.

A total of seven natural frequencies can be identified from the FRFs shown in Figure 9a. The reference point in the given example is placed approximately in the middle of the beam. This location (given the free-free boundary conditions) in terms of the translations for odd eigenfrequencies represents the position of anti-nodes, where the response exhibits extreme amplitudes. On the contrary, for even eigenfrequencies the reference point is placed in the proximity of the nodes.

From the translational FRFs, therefore it is possible to clearly identify the natural frequencies that correspond to the odd vibration modes, while the natural frequencies that correspond to the even vibration modes are not so clearly visible. A vice-versa situation can be observed for the rotational sensor, with odd natural frequencies even more difficult to detect, since the noise level of the rotational sensor is relatively high, compared to the translational accelerometer. The driving-point measurement is shown in Figure 9b. Since the even modes are



(a)



(b)

Figure 9: Measured FRFs: (a) Point 0; (b) Driving point.

not excited during the driving-point measurement, the natural frequencies corresponding to the even modes are not visible in the case of either translational or rotational FRFs.

4.4. Steps 2 and 3: Pole identification and pole mixing

The separate identification of complex eigenvalues was performed on a set of translational and rotational FRFs using the LSCF. The corresponding stabilization diagrams are shown in Figure 10, with the stable poles being indicated by green-cross markers.

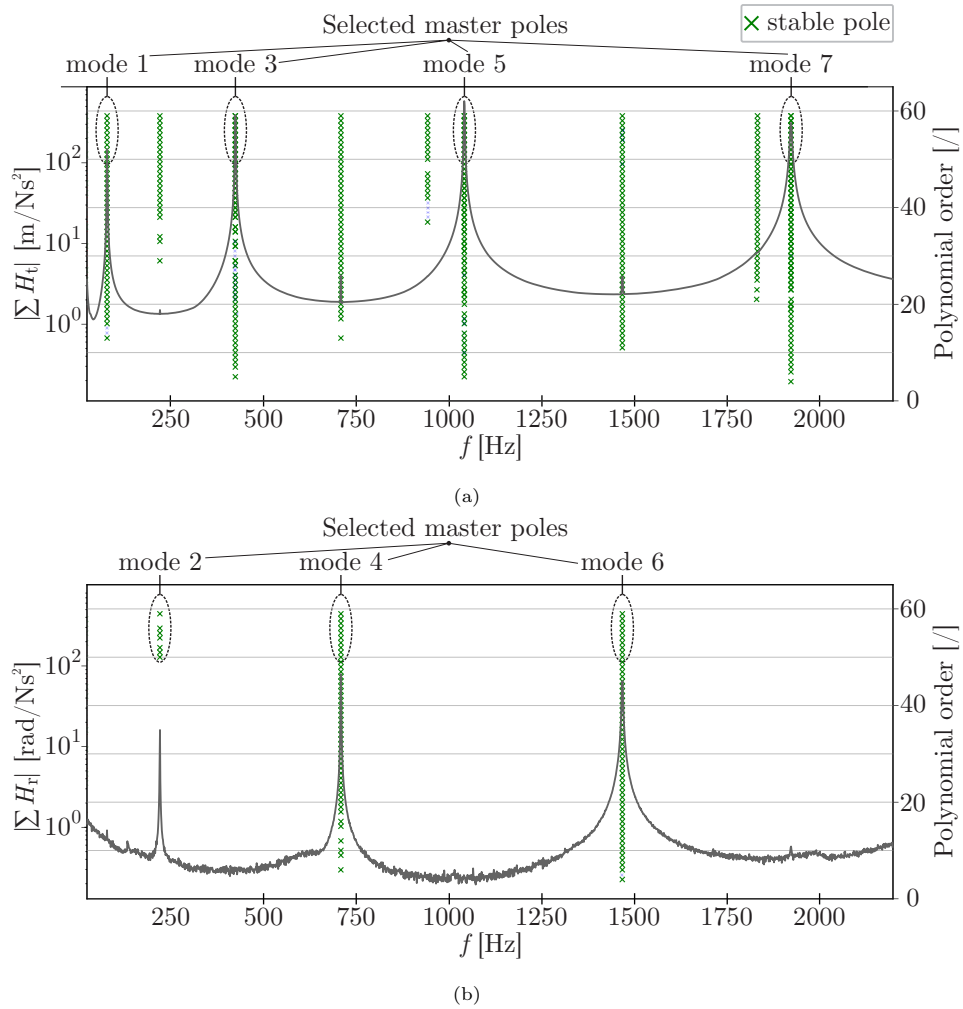


Figure 10: Stabilization diagram: (a) Translation; (b) Rotation.

As is apparent from Figure 10a, stabilization is achieved at both the master and slave translational resonance peaks; therefore, all the natural frequencies and the corresponding damping ratios can be identified. However, this is not the case with the rotational diagram, presented in Figure 10b, where the stabilization can only be observed for odd vibration modes. As labeled in Figures 10a and 10b, all the high response resonances were selected as the master peaks and the corresponding master poles represent the basis for a further modal param-

eter estimation.

4.5. Steps 4 and 5: Standard and hybrid identification of modal constants

The pre-calculated set of master poles was adopted within the estimation of the modal constants and the standard LSFD method used for both the translational and rotational sets of FRFs separately.

Within the hybrid LSFD method, when considering translational measurements, the hybrid approach was applied to estimate even (slave) rows of the matrix \mathbf{A} (see Figure 5) that were not clearly detectable in the translational FRFs. The corresponding even rotational rows of the MCs, which were clearly observable from the rotational FRFs, served as the master rows. A comparison of the identified modal constants² obtained using the standard and the hybrid LSFD is shown in Figure 11.

In addition to the translation-slave and the hybrid modal constants, the rotational master modal constants are also presented. They are included to represent the shape of the modal constants that is imposed on the translation-slave modal constants in the hybrid estimation. It is shown that inconsistent modal constants can be obtained for slave rows when the standard LSFD is considered. This is most obvious for the second vibration mode. Nevertheless, a fairly good match can be observed for the fourth and sixth vibration modes. In addition to the graphical comparison, the Modal Assurance Criterion (MAC) [32] is calculated with regards to the analytical mode shape prediction for a homogenous free-free supported beam [33]. The results are presented in Table 1, showing a significant improvement in the hybrid procedure, compared to the standard approach.

²Relative phase shifts between individual points for the structure under consideration turn out to be either close to 0° or 180° , therefore stationary depiction of complex vectors is used.

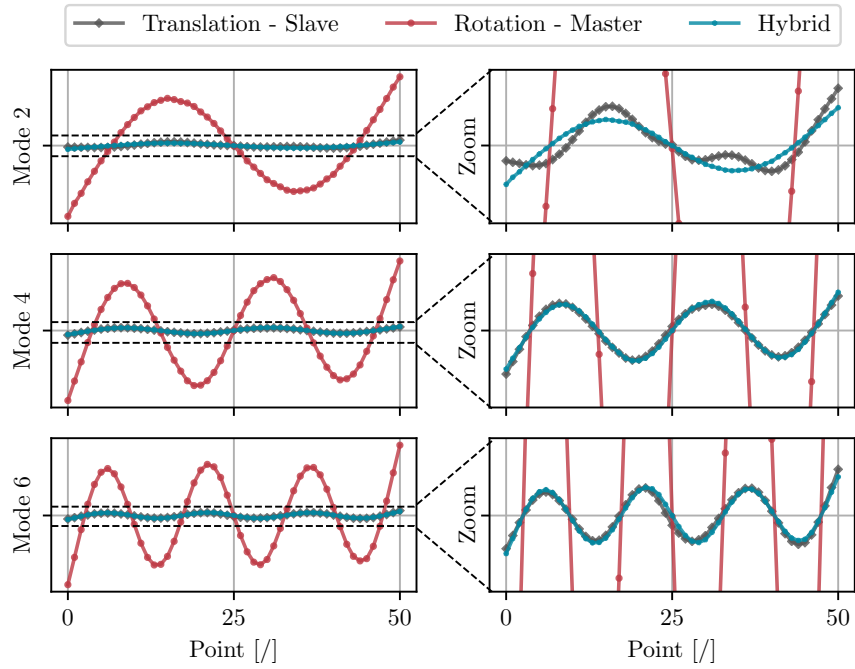


Figure 11: Estimated modal constants for even natural frequencies.

Table 1: Even modes: MAC values - compared to the analytical prediction.

	Mode 2	Mode 4	Mode 6
			
MAC (Slave, Analytical)	0.76	0.87	0.89
MAC (Hybrid, Analytical)	0.99	0.98	1.00

However, when the mass-normalized mode shapes are considered³, a more

³It should be noted that also the relationship between the acceleration and the receptance is to be considered, in order to obtain mass-normalized mode shapes.

significant difference between the standard and the hybrid LSF methods can be observed. The reference mode shape was obtained by placing the reference point 40 mm from the centroid of the beam to avoid any problems with node proximity. As an example, translational and hybrid variation of mass-normalized mode shapes for the second and fourth vibration mode are given, as shown in Figure 12. In both cases, normalization was performed by considering the corresponding driving point values of estimated modal constants.

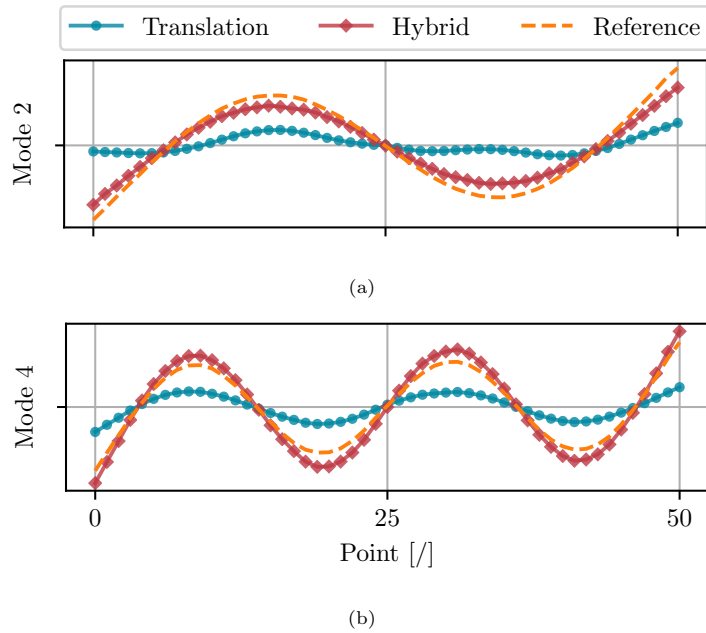


Figure 12: Normalized modal shapes: (a) Mode 2; (b) Mode 4.

The reason for discrepancies in normalization can be attributed to the influence of the estimated driving-point values. Since the driving-point for the even translational mode shapes is located near the nodes, close-to-zero values are expected. Therefore, even a small inconsistency in the evaluation of the modal constants can have a significant impact on the scaling of the mass-normalized mode shapes. When using the hybrid LSF, the estimated driving-point value appears to be more accurate since the contribution of the rotational mode shape

to the modal constant value is not subjected to the node-proximity problem. This results in a more accurate normalization, which can be confirmed by the reference mass-normalized mode shape.

In the case of rotational measurements, the hybrid approach was applied to deduce the odd (slave) rows of matrix \mathbf{A} . The advantage of the used rotational sensor, compared to the translational one, is in the insensitivity to the offset from the centroid axis as there is also a lower base-strain and cross-axis sensitivity due to the unique placement of the piezo-crystals. On the other hand, its high noise level leads to several problems, starting with the inability to make a low-response pole identification. Without taking into account the poles from the translational measurement in *Step 3*, the identification of the modal constants would not even be possible. However, even by using the set of master poles in correlation with the standard LSFD, a significant effect of the noise can be observed from the identified modal constants as shown in Figure 13.

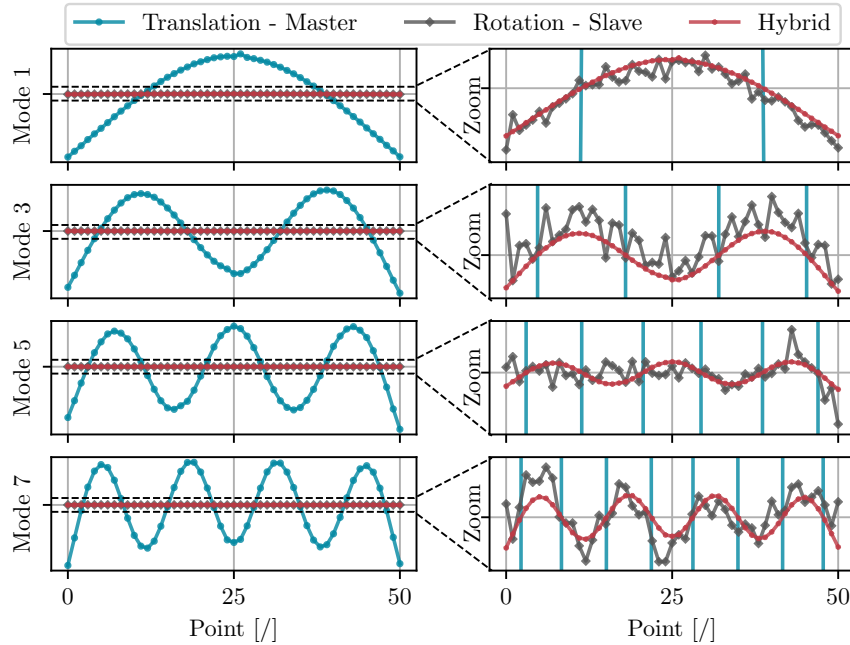


Figure 13: Estimated modal constants for odd natural frequencies.

The hybrid LSFD estimates of the odd (slave) vibration-mode-related modal constants; however, show a significant improvement in the consistency, which is also evident from the quantitative comparison in Table 2.

Table 2: Odd modes: MAC values - compared to the analytical prediction.

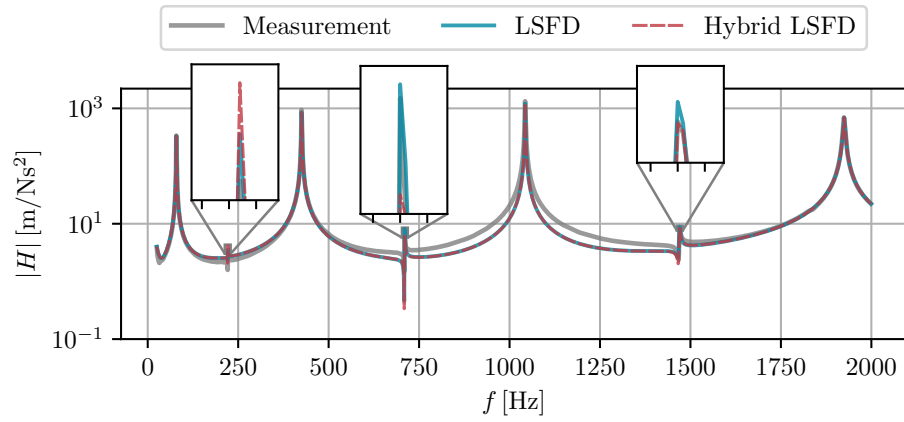
	Mode 1	Mode 3	Mode 5	Mode 7
				
MAC (Slave, Analytical)	0.83	0.26	0.16	0.42
MAC (Hybrid, Analytical)	1.00	0.99	0.96	0.99

4.6. Step 6: FRF reconstruction

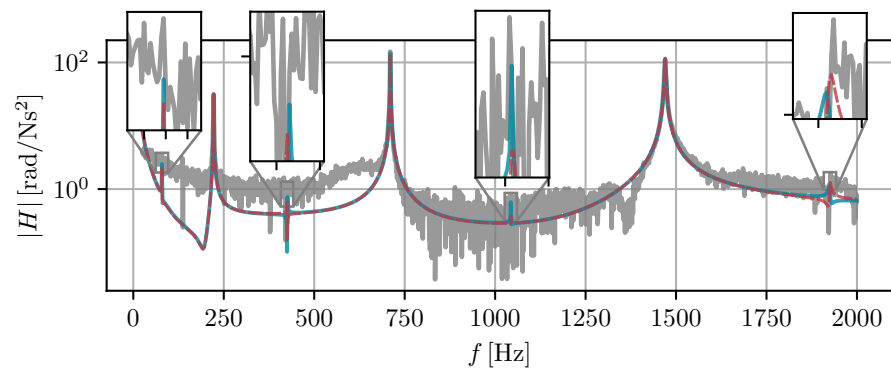
In the following section, standard and hybrid type of reconstructed FRFs at points 0 in 25 are compared to the actual measurement carried out at these points. In addition to the graphical representation, a coherence criterion [34] is also used for quantitative comparison. Since the hybrid LSFD differs from the standard LSFD only in the evaluation of slave-peak-related modal constants, no discrepancies in the master peak amplitudes are expected.

Accordingly, the quantitative comparison parameter (QCP) is calculated as the average measurement-reconstruction coherence criterion [34] value in the ± 10 Hz bandwidth around the slave-peak-related natural frequencies.

A comparison of the FRFs for the translational and rotational response at Point 0 is presented in Figure 14 and the corresponding values of the QCP values are given in Table 3.



(a)



(b)

Figure 14: FRF reconstruction - Point 0: (a) Translation; (b) Rotation.

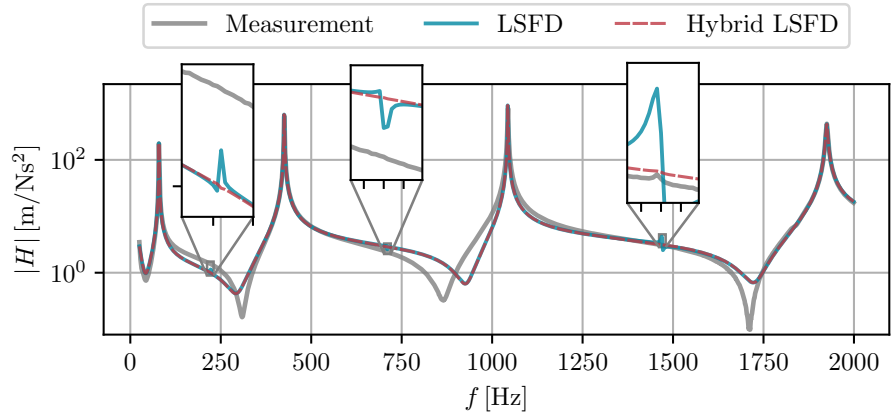
Table 3: QCP based on measurement-reconstruction coherence criterion at Point 0.

	Standard LSFDF	Hybrid LSFDF
QCP Translation - Even natural frequencies	94.4%	94.1%
QCP Rotation - Odd natural frequencies	73.5%	72.0%

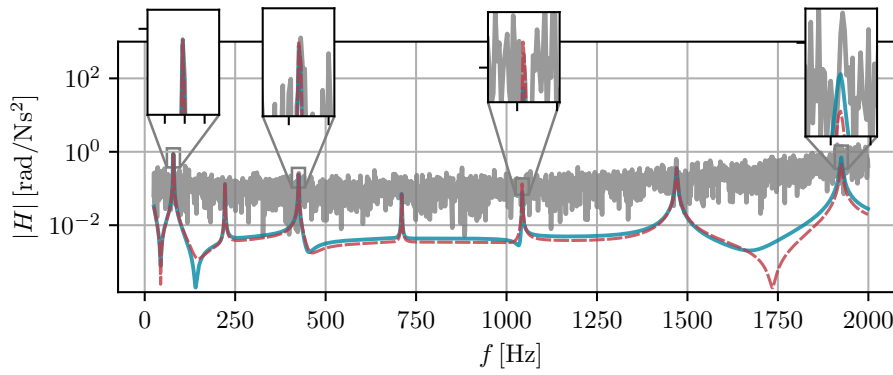
Compared to the hybrid LSFD reconstructions, a slightly better agreement between the measurement and the standard LSFD reconstruction can be observed for both, translational and rotational response. This is expected due to the local nature of the modal parameter estimation that is performed on essentially uncorrelated degrees of freedom (DoFs). The hybrid LSFD, however, introduces a correlation between the DoFs imposed by the corresponding mode shape (obtained by a different sensor) that has no node-proximity problems. Therefore, the hybrid LSFD reconstruction at the expense of a minimal reduction in the coherence towards measurement, represents physically consistent information with regards to the remaining set of FRFs even in the slave-peak related frequency bandwidth.

The driving-point comparison of FRFs is presented in Figure 15 and the corresponding values of the QCP values are given in Table 4. As already observed, the identified amplitudes of the translational modal constants (Figure 15a), obtained by the standard LSFD, appear to have inaccurate (too high) values at low response peaks. This leads to spurious peaks in the reconstructed FRF at the corresponding natural frequencies. However, this is not the case with the reconstruction obtained by the hybrid LSFD, where rotational data is used as a basis for the modal constants identification. The QCP value for both reconstructions is practically identical.

When examining the measured rotational FRF for the driving point in Figure 15b, practically all the identified resonance peaks are located below the noise floor. The pre-calculated set of mixed poles can still be adopted and the standard/hybrid LSFD least-squares procedure is performed. However, in the standard approach the modal constants for all the modes are identified with respect to the rotational measurements. Within the hybrid approach, the only change occurs at odd natural frequencies, where the proportionality to the translational row of modal constants is imposed before performing the least-squares procedure. In this case, both the standard and the hybrid FRF reconstruction give practically the same results, which is apparent from both, the graphical and quantitative comparisons in Figure 15 and Table 4, respectively.



(a)



(b)

Figure 15: FRF reconstruction - Driving point: (a) Translation; (b) Rotation.

Table 4: QCP based on measurement-reconstruction coherence criterion at Point 25.

	Standard LSF	Hybrid LSF
QCP		
Translation - Even natural frequencies	96.7%	96.6%
QCP		
Rotation - Odd natural frequencies	62.3%	62.5%

5. Conclusions

In this paper a new approach to modal identification in the case of the near-to-node experimental response model is presented. First, a reliable complex eigenvalue identification is ensured, using a combination of master-peak-related data. Next, a hybrid LSF method is proposed in order to improve the consistency of the estimated modal constants, also effecting the modal-shape normalization and the FRF reconstruction. Finally, an experimental study demonstrates the efficiency and accuracy of the proposed approach. The use of related experimental response models appears to be a convenient alternative to the established multi-reference approach, whereas the use of the hybrid LSF method appears to be a useful tool to improve the evaluation of modal constants.

Compared to the modal parameters that can be identified by separate analysis of the acquired (different) response models, with the proposed hybrid approach a FRF reconstruction of unidentifiable resonance peaks is enabled. Moreover, a methodology is introduced, to increase the consistency of the unreliable estimates. Provided that one of the used response-excitation pairs exhibits complementary properties, the mass normalization of the mode shapes is also possible.

The study in this paper is limited to the use of different response models when a single-row response model is obtained at a reference measurement point. However, the same concept can be applied with the use of different types of excitation in the case of column-based measurements and even with the established multi-reference measurements, to rectify the estimated modal constants and the reconstructed FRFs.

When performing experimental modal analysis on real structures, various problems can arise, requiring to use case-specific methods in order to be managed. Therefore, some different or even additional steps to the presented procedure may be required to provide successful modal identification, however the basic approach of using multiple related response models remains the same.

Acknowledgements

The authors acknowledge partial financial support from the core research funding P2-0263 and the applied research project L2-1837, both financed by ARRS, the Slovenian research agency.

References

- [1] P. Avitabile, *Modal testing: a practitioner's guide*, John Wiley & Sons, 2017.
- [2] A. Elliott, A. Moorhouse, G. Pavić, Moment excitation and the measurement of moment mobilities, *Journal of sound and vibration* 331 (11) (2012) 2499–2519.
- [3] Y. Champoux, V. Cotoni, B. Paillard, O. Beslin, Moment excitation of structures using two synchronized impact hammers, *Journal of sound and vibration* 263 (3) (2003) 515–533.
- [4] R. Farshidi, D. Trieu, S. Park, T. Freiheit, Non-contact experimental modal analysis using air excitation and a microphone array, *Measurement* 43 (6) (2010) 755–765.
- [5] V. Ondra, B. Titurus, Theoretical and experimental modal analysis of a beam-tendon system, *Mechanical Systems and Signal Processing* 132 (2019) 55–71.
- [6] S. Sels, S. Vanlanduit, B. Bogaerts, R. Penne, Three-dimensional full-field vibration measurements using a handheld single-point laser doppler vibrometer, *Mechanical Systems and Signal Processing* 126 (2019) 427–438.
- [7] J. Javh, J. Slavič, M. Boltežar, High frequency modal identification on noisy high-speed camera data, *Mechanical Systems and Signal Processing* 98 (2018) 344–351.

- [8] A. Drozg, J. Rogelj, G. Čepon, M. Boltežar, On the performance of direct piezoelectric rotational accelerometers in experimental structural dynamics, *Measurement* 127 (2018) 292–298.
- [9] W. W. I. Mirza, M. A. Rani, M. Yunus, R. Febrina, M. Sani, Estimating rotational FRFs of a complex structure using FE model updating, mode expansion and FRF synthesis method, *IOP Conference Series: Materials Science and Engineering* 807 (2020) 012045.
- [10] F. Dos Santos, B. Peeters, J. Lau, W. Desmet, L. Góes, An overview of experimental strain-based modal analysis methods, in: *Proceedings of the International Conference on Noise and Vibration Engineering (ISMA)*, Leuven, Belgium, 2014.
- [11] T. Kranjc, J. Slavič, M. Boltežar, The mass normalization of the displacement and strain mode shapes in a strain experimental modal analysis using the mass-change strategy, *Journal of Sound and Vibration* 332 (26) (2013) 6968–6981.
- [12] P. Guillaume, P. Verboven, S. Vanlanduit, Frequency-domain maximum likelihood identification of modal parameters with confidence intervals, in: *Proceedings of the international seminar on modal analysis*, Vol. 1, Katholieke Universiteit Leuven, 1998, pp. 359–366.
- [13] P. Guillaume, L. Hermans, H. Van der Auweraer, Maximum likelihood identification of modal parameters from operational data, in: *Proceedings of the 17th International Modal Analysis Conference (IMAC17)*, 1999, pp. 1887–1893.
- [14] H. Van Der Auweraer, W. Leurs, P. Mas, L. Hermans, Modal parameter estimation from inconsistent data sets, in: *Proceedings of SPIE-The International Society for Optical Engineering*, Vol. 4062, 2000.
- [15] B. Peeters, H. Van der Auweraer, P. Guillaume, J. Leuridan, The polymax

- frequency-domain method: a new standard for modal parameter estimation?, *Shock and Vibration* 11 (3, 4) (2004) 395–409.
- [16] X.-J. Yao, T. H. Yi, C. Qu, H. N. Li, Blind modal identification in frequency domain using independent component analysis for high damping structures with classical damping, *Computer-Aided Civil and Infrastructure Engineering* 33 (1) (2018).
- [17] X.-J. Yao, T. H. Yi, C. Qu, H. N. Li, Blind modal identification using limited sensors through modified sparse component analysis by time-frequency method, *Computer-Aided Civil and Infrastructure Engineering* 33 (9) (2018).
- [18] T.-H. Yi, X.-J. Yao, C.-X. Qu, H.-N. Li, Clustering number determination for sparse component analysis during output-only modal identification, *Journal of Engineering Mechanics* 145 (1) (2019).
- [19] D. Kientzy, M. Richardson, K. Blakely, Using finite element data to set up modal tests, *Sound and Vibration Magazine* 23 (6) (1989) 16–23.
- [20] D. C. Kammer, Sensor placement for on-orbit modal identification and correlation of large space structures, *Journal of Guidance, Control, and Dynamics* 14 (2) (1991) 251–259.
- [21] C. Papadimitriou, Optimal sensor placement methodology for parametric identification of structural systems, *Journal of sound and vibration* 278 (4-5) (2004) 923–947.
- [22] C. Stephan, Sensor placement for modal identification, *Mechanical Systems and Signal Processing* 27 (2012) 461–470.
- [23] N. M. M. Maia, J. M. M. e Silva, *Theoretical and experimental modal analysis*, Research Studies Press, 1997.
- [24] R. Lin, J. Zhu, On the relationship between viscous and hysteretic damping models and the importance of correct interpretation for system identification, *Journal of Sound and Vibration* 325 (1-2) (2009) 14–33.

- [25] A. Drozg, G. Čepon, M. Boltežar, Full-degrees-of-freedom frequency based substructuring, *Mechanical Systems and Signal Processing* 98 (2018) 570–579.
- [26] G. T. Mase, R. E. Smelser, J. S. Rossmann, *Continuum mechanics for engineers*, CRC press, 2020.
- [27] D. J. Ewins, *Modal testing: theory and practice*, Vol. 15, Research studies press Letchworth, 1984.
- [28] C.-X. Qu, T.-H. Yi, H.-N. Li, B. Chen, Closely spaced modes identification through modified frequency domain decomposition, *Measurement* 128 (2018) 388–392.
- [29] S. Wei, S. Chen, Z. Peng, X. Dong, W. Zhang, Modal identification of multi-degree-of-freedom structures based on intrinsic chirp component decomposition method, *Applied Mathematics and Mechanics* 40 (12) (2019) 1741–1758.
- [30] M. Dumont, N. Kinsley, Rotational accelerometers and their usage in investigating shaker head rotations, in: *Sensors and Instrumentation*, Volume 5, Springer, 2015, pp. 85–92.
- [31] J. Maierhofer, A. El Mahmoudi, D. J. Rixen, Development of a low cost automatic modal hammer for applications in substructuring, in: *Dynamic Substructures*, Volume 4, Springer, 2020, pp. 77–86.
- [32] R. J. Allemang, The modal assurance criterion—twenty years of use and abuse, *Sound and vibration* 37 (8) (2003) 14–23.
- [33] S. S. Rao, *Mechanical Vibrations*, in SI Units, Global Edition, Pearson, London, 2017.
- [34] M. van der Seijs, D. van den Bosch, D. J. Rixen, D. de Klerk, An improved methodology for the virtual point transformation of measured frequency response functions in dynamic substructuring, *Proceedings of the 4th COMPDYN* (2014).